Int. J. Electrochem. Sci., 13 **(2018)** 1577 – 1593, doi: 10.20964/2018.02.01

International Journal of
ELECTROCHEMICAL
SCIENCE
www.electrochemsci.org

Application of an Acid Extract of Barley Agro-Industrial Waste as a Corrosion Inhibitor for Stainless Steel AISI 304 in H_2SO_4

Larissa Aparecida Corrêa Matos[1], *Mariane Coussian Taborda*[1], *Guilherme José Turcatel Alves*[1], *Maico Taras da Cunha*[1], *Everson do Prado Banczek*[1], *Marilei de Fátima Oliveira*[2], *Eliane D'Elia*[3], *Paulo Rogério Pinto Rodrigues*[1*]

[1] GPEL® Laboratório do Grupo de Pesquisas em Eletroquímica, Departamento de Química, Universidade Estadual do Centro Oeste, Rua Simeão Camargo Varela de Sá 03, 85040-080, Vila Carli, Guarapuava, Paraná, Brasil.
[2] UTFPR, Avenida Professora Laura Pacheco Bastos 800, 85053-525, Industrial, Guarapuava, Paraná, Brasil.
[3] Departamento de Química Inorgânica, Instituto de Química, UFRJ, Avenida Athos da Silveira Ramos 149, Centro de Tecnologia, Bloco A, Laboratório 634A, Cidade Universitária, Rio de Janeiro, 21941-909, Rio de Janeiro, Brasil.
[*]E-mail: prprodrigues@unicentro.br

Received: 25 August 2017 / *Accepted:* 17 November 2017 / *Published:* 28 December 2017

Corrosion inhibitors are commonly used to reduce the effects of corrosive processes in metallic materials. However, many compounds are toxic and expensive and have negative effects on the environment. There is growing interest in replacing petroleum inhibitors with biodegradable inhibitors, such as plant extracts. Barley agro-industrial waste (AW) is a source of compounds with great inhibitor activity, and its use is desirable for minimizing the amount of AW. The aim of this paper is to demonstrate the application of an AW extract as a corrosion inhibitor for stainless steel AISI 304 in H_2SO_4. The efficiency of this acid extract was evaluated by weight loss measurements, scanning electron microscopy (SEM) analysis, open circuit potential (OCP) measurements, electrochemical impedance spectroscopy (EIS), and potentiodynamic polarization curves (PP). The proposed extract exhibited an inhibition efficiency of up to 97% and was physically adsorbed in the metallic surface. The SEM images indicated that the addition of the extract decreased metal oxidation. The electrochemical results for steel in the presence of the AW extract acted as a mixed-type inhibitor, likely changing the cathodic mechanism reaction on the uncovered surface. The AW extract can thus be used as an organic corrosion inhibitor.

Keywords: green inhibitor, sustainability, acid inhibition

1. INTRODUCTION

Stainless steel is extensively used in industrial settings due to its corrosion resistance properties [1]. The great cost–benefit of stainless steel can be attributed to its oxide layer, which is a mixture of iron and chromium oxides and hydroxides [2]. However, such steel is susceptible to corrosion processes, mainly in acidic media [3].

To reduce the effects of corrosion in acidic media, corrosion inhibitors are added to the electrolytic media [3–7]. Inhibitors are substances that promote the partial blockage of the metallic surface, even at low concentrations. They can act through chemical or physical adsorption, the formation of an oxide layer, or the modification of the corrosive media [8]. The use of inhibitors is one of the most practical anti-corrosion methods, mostly in acidic media, where it is necessary to prevent metallic dissolution and acid consumption [9].

The inhibition efficiency of the compounds depends on their physicochemical properties. Most of the organic inhibitors contain polar functional groups, with aromatic rings, heteroatoms, and π electrons that are adsorbed in the metallic surface [1,4]. Organic compounds, such as azoles and phenylazoles, are commonly used as inhibitors [1,8,10]. These compounds present great anti-corrosion efficiency, but mostly cause undesirable effects due to their toxicity to humans, environmental deterioration, and high cost of application [9].

There is great interest in replacing these toxic organic compounds with ecological and biodegradable alternatives. The technological application of agro-industrial and food waste has been extensively studied, for both reducing the waste itself and increasing its value in the agro-industry [9]. Natural compounds, such as feed peels and plant extracts, have become a viable alternative due to their availability and high protein, polysaccharide, polycarboxylic acid, and alkaloid contents, which have inhibitory abilities [11,12]. The extracts have great viability because they can be obtained with low cost and through simple acidic, neutral, or basic extraction methods [4,9,13,14].

Aqueous plant extracts are viewed as a source of naturally biodegradable organic compounds and can be extracted by simple procedures, resulting in high efficiency [4]. Coffee extracts, garlic husks, fruit peels, *Ilex paraguariensis*, and *Poinciana pulcherrima* were studied and showed great efficiency against the corrosive processes of HCl in carbon steel [4,9,12–14]. For stainless steel, efficient results were obtained with the use of *Salvia officinalis* leaves and khillah extract [5,15].

Agro-industrial activities produce thousands of tons of waste globally. Much of these wastes are used as animal feed [16]. These wastes contain great quantities of nutrients and antioxidant compounds, which can be used to obtain chemical substances with inhibitory activity, adding value to the waste, generating environmental benefits, and improving the economic viability of the responsible management of agro-industrial waste [17].

Barley is the fourth world crop, generating thousands of tons of waste per year. Its composition includes a high content of natural antioxidants, such as phenolic compounds. Moreover, it is a rich source of amino acids, ascorbic acid, and glutathione, and as such is incorporated into many food products and diets [18]. This paper aims to study the use of an acid extract from the agro-industrial waste (AW) of barley as a green corrosive inhibitor for stainless steel AISI 304 in 1.5 mol L^{-1} H_2SO_4.

2. MATERIALS AND METHODS

2.1. Preparation of the metallic substrates

The metallic substrates used were AISI 304 stainless steel samples, with chemical compositions of 18.49 Cr, 0.68 Mn, 8.40 Ni, and 72.43 Fe (% m/m). The stainless steel surfaces were successively abraded with #320, #400, #600, and #1200 SiC paper, washed with distilled water, and air dried before each test.

2.2. Barley agro-industrial waste characterization

Barley agro-industrial waste (AW) corresponds to the remaining products of the malting process. In this process, the residue is the non-germinated barley that will not become malt. This residue, known as malt bagasse, has a composition with a nutritional and technological potential that should be harnessed. Barley bark and non-germinated barley, whose production reaches up to 3 tons daily, is typically discarded as animal feed. However, this is undesirable due to its low digestibility. This waste is presented in bran form with high humidity and is known to be rich in proteins (10%), carbohydrates (73%), and lipids (3.1%), beyond digestible nutrients [19]. The waste is collected, dried, and grounded to avoid fermentation.

The AW used in the experiments in this study was metallized using Quorum Q150R ES equipment. The AW was analyzed by scanning electron microscopy (SEM) in a Tescan VEGA3 microscope, with a 10 keV tension. The elementar composition was realized by energy dispersion spectroscopy (EDS) in an Oxford X-act spectrometer, at 10 keV.

The AW was submitted to combustion in a Pelkin Elmer 2400 series II analyzer, in a pure oxygen atmosphere, to determine the chemical composition by elemental analysis. The gases resulting from the combustion were quantified in a thermal conductivity detector.

2.3. Extract preparation

The AW acid extracts were obtained by the addition of 5 g of barley waste in sufficiently concentrated H_2SO_4 to obtain 1 L of 1.5 mol L^{-1} H_2SO_4 solution for 6 h. The resultant mixture was filtered, and the filtered solution was directly used for experimental purpose as stock solution (5 g L^{-1}). The other concentrations of the AW acid extract (1, 2, 3, and 4 g L^{-1}) were prepared by dilution of the stock solution [20].

2.4. Weight loss experiments

The weight loss experiments were realized according to the ASTM G31/72 standard [21], in a 22 ± 2 ºC TE-2005 TECNAL thermostatic bath, at GPEL®, Unicentro. The stainless steel samples were immersed for 2 h in 50 mL of H_2SO_4 in the presence and absence of different concentrations of

the AW acid extract. The weight loss measurements were realized in an analytic balance with 0.1-mg accuracy. The corrosion rate (v_{corr}) was calculated according to equation 1 [8]:

$$v_{corr} = \frac{\Delta m}{A \times t} \quad (1)$$

where A corresponds to the surface area (cm^2), $\Delta m = m_f - m_i$, where m_f is the final mass and m_i is the initial mass of the metallic sample before the experiment (mg), and t is the immersion time (h).

The inhibitory efficiency (IE) was calculated according to equation 2 [8]:

$$IE = \frac{v_{corr,0} - v_{corr}}{v_{corr,0}} \times 100 \quad (2)$$

where $v_{corr,0}$ and v_{corr} are the corrosion rate in the absence (blank) and presence of AW, respectively.

The temperature effect was evaluated by the test in the absence and presence of the AW acid extract, with concentrations of 1 to 5 g L^{-1}, in thermostatic baths at 32 ºC, 42 ºC, and 52 ºC.

2.5. Surface analysis

The metallic samples were evaluated by Tescan VEGA 3 scanning electron microscopy (SEM) and energy dispersive spectroscopy (EDS) in an Oxford X-act spectrometer, allowing for the determination of the chemical composition of the metallic samples after immersion in the AW acid extract. The accelerating voltage was 20 kV.

2.6. Electrochemical procedure

The electrochemical procedure was realized in an Autolab PGSTAT302N potentiostat, with an electrochemical three-electrode cell of 100 mL. For the working electrodes, samples of AISI 304 stainless steel with an area of 0.68 cm^2 were used; for the counter electrodes, a platinum wire with a large superficial area was applied; for the reference electrode, a mercurous sulphate electrode (MSE) was used and an electrolyte solution of 1.5 mol L^{-1} H_2SO_4 containing the AW acid extract was applied.

In all experiments, the stainless steel was stabilized until the OCP reached approximately 2 h of immersion in the electrolyte.

Polarization curves were obtained in both directions (anodic and cathodic) from the OCP, applying a cathodic overpotential (η_c) of -1.0 V and an anodic overpotential (η_a) of +1.8 V, with a scanning rate of 1.0 mV s^{-1}. The corrosion parameters, such as corrosion potential (E_{corr}), corrosion current density (j_{corr}), and anodic and cathodic Tafel slopes (βa and –βc, respectively), were obtained from Tafel extrapolation.

The inhibitory efficiency was obtained from equation 3:

$$IE = \frac{j_{corr,0} - j_{corr}}{j_{corr,0}} x100 \quad (3)$$

where $j_{corr,0}$ and j_{corr} are the corrosion current density of steel, with and without the AW acid extract, respectively, in the H_2SO_4 solution.

The system was also evaluated by electrochemical impedance spectroscopy (EIS). A potential perturbation of ±10 mV was applied from the OCP in frequencies from 10 kHz to 0.01 Hz. The R_{ct} values were used to calculate the inhibitory efficiency, according to equation 4:

$$IE = \frac{R_{ct} - R_{ct,0}}{R_{ct}} x100 \ (4)$$

where $R_{ct,0}$ and R_{ct} correspond to the charge transfer resistance in the absence and presence of the AW extract, respectively.

3. RESULTS AND DISCUSSION

3.1. Barley agro-industrial waste characterization

Figure 1 shows that the AW morphology is typically fibrous, alveolar and presents irregular rods resulting from the milling process. EDS mapping is presented in Figure 2.

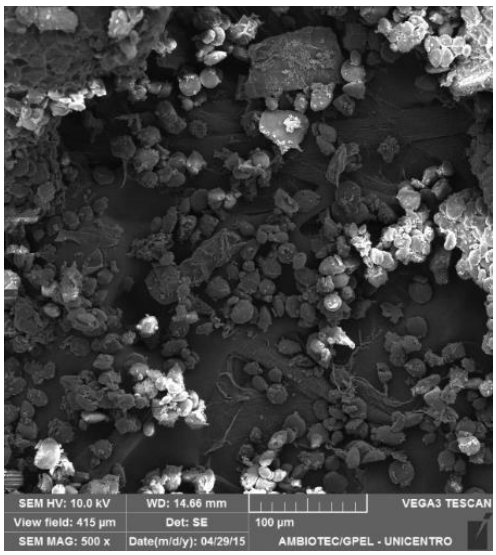

Figure 1. SEM image of crude barley agro-industrial waste. 500x zoom.

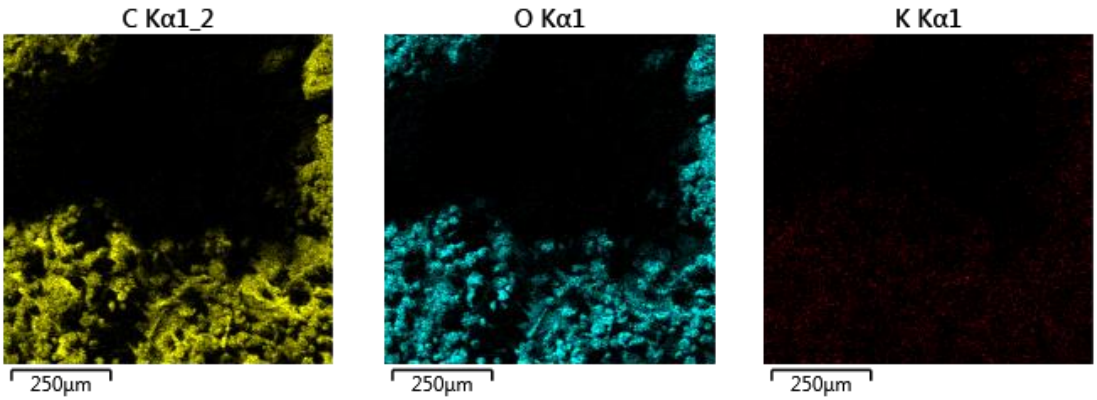

Figure 2. EDS mapping of agro-industrial metallized waste.

Table 1. Elemental analysis of the AW.

Element	% / m/m
Carbon	41.2 ± 0.54
Hydrogen	6.89 ± 0.03
Nitrogen	1.45 ± 0.18

From Figure 2, it is noted that the AW sample presents Kα1 lines to carbon, oxygen, and potassium, in lower intensities. The proportions of these elements are 64.7%, 34.9%, and 0.26%, respectively. Table 1 presents the chemical composition of the AW obtained by elemental analysis.

Table 1 demonstrates that great quantities of carbon are present in the AW. From data shown in Figure 2 and Table 1, it can be claimed that the main composition of the waste is C, N, O, H, N, which are all features of organic compounds, and K.

The presence of N and O in the waste's organic compounds is a potential source of electron pairs available to its adsorption onto the metallic surface, promoting the partial blockage of the metal and the consequent inhibition of corrosion in acidic media [13]. As this waste presents proteins in high quantities (10%, approximately), which in turn presents both N and O atoms, it is possible to propose this compound's class as inhibitory molecules. The abundant compounds in the organic waste could be extracted by different methodologies and used as corrosion inhibitors in other metal/corrosive media systems [4].

3.2. Weight loss experiments

Table 2 presents the results of the weight loss measurements on AISI 304 stainless steel corrosion in 1.5 mol L^{-1} H_2SO_4. The weight loss method of monitoring the corrosion rate and inhibition efficiency is useful because of its simple application and reliability [5]. The corrosion rate (ν_{corr}) of AISI 304 stainless steel in 1.5 mol L^{-1} H_2SO_4 obtained without extract was 0.9165 mg cm^{-2} h^{-1}. This value is very close to the literature results as obtained for 304 stainless steel in 1.0 mol L^{-1} HCl (1.25 mg cm^{-2} h^{-1}) [22].

Table 2. Corrosion rate and inhibitory efficiency of the AW acid extract for AISI 304 stainless steel coupons in 1.5 mol L^{-1} H_2SO_4.

[AW] / g L^{-1}	ν_{corr}/ mg cm^{-2} h^{-1}	I.E. / %
0	0.9165	-
1	0.2019	78.0
2	0.1034	88.7
3	0.08542	90.7
4	0.06024	93.4
5	0.02610	97.1

The values shown in Table 2 show that the corrosion rate of stainless steel decreased with the addition of the extract. Higher concentrations of the acid extract promoted higher surface blocking, as demonstrated by the increase in the inhibitory efficiency.

The solvent molecules are also adsorbed at the metal/solution interface during corrosion inhibition of metals. According to the Bockris-Devanathan-Müller model, the adsorption process in aqueous solution can be regarded as a substitution process between the organic compounds in the aqueous phase [Org(sol)] and water molecules at the electrode surface [$H_2O_{(ads)}$] [23]:

$$Org_{(sol)} + x\ H_2O_{(ads)} \rightarrow Org_{(ads)} + x\ H_2O_{(sol)}$$

where x is the number of water molecules replaced by one organic inhibitor.

The interaction between the inhibitor and the metallic surface can be described by the adsorption isotherms. The fraction of the surface covered (θ) by adsorbed molecules is directly proportional to the inhibitory efficiency. Several models were used for this purpose (Langmuir, Freundlich, Temkin, Flory-Huggins, El-Awady), and the results obtained from weight loss measurements were used to describe the adsorption process, according to equations 5-10 [23]:

$$\theta = I.E./100 \quad (5)$$

$$Langmuir: \frac{c}{\theta} = \frac{1}{K} + c \quad (6)$$

$$Freundlich: \log\theta = \log K + \frac{1}{n}\log c \quad (7)$$

$$Temkin: \theta = \left(-\frac{2.303}{2a}\right)\log K + \left(-\frac{2.303}{2a}\right)\log c \quad (8)$$

$$Flory - Huggins: \log\left(\frac{\theta}{c}\right) = \log K + x\log(1-\theta) \quad (9)$$

$$El - Awady: \log\left(\frac{\theta}{1-\theta}\right) = \log K + y\log c \quad (10)$$

where c is the concentration, K is the adsorption constant, 1/n is the Freundlich exponent, a is the lateral parameter of interaction between adsorbed molecules, x is the number of adsorbed water molecules substituted by inhibitor molecules, and y is the number of adsorbed molecules in an active site [23-27].

The studied isotherms showed correlation coefficients of 0.998, 0.952, and 0.959 for the Langmuir, Freundlich, and Temkin models, respectively.

Table 3. Adsorption parameters obtained with the AW acid extract on the corrosion inhibition of AISI 304 stainless steel.

Isotherm	**R^2**	**y = a + bx**
Langmuir	0.998	y = 0.323 + 0.977 x

The best fitting was obtained by Langmuir adsorption isotherm. Table 3 shows the adsorption parameters for the Langmuir isotherm with an R^2 of 0.998 and a slope close to the unit (0.977), leading to an adsorption equilibrium constant of 3.09 L g^{-1} for the AW acid extract.

The Langmuir isotherm assumes that the molecules, likely the proteins present in the bagasse of the malt, adsorb onto the surface without interactions between the adsorbed molecules [4]. As the extract components responsible for the inhibition process do not have a known molecular mass, the calculation of thermodynamic parameters is unachievable [13,28].

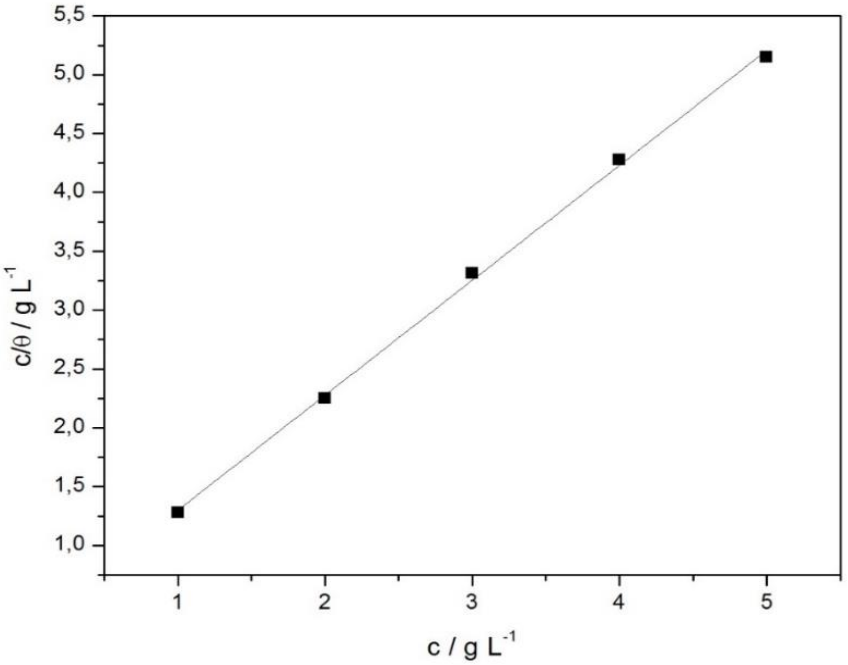

Figure 3. Langmuir adsorption isotherm of the AW acid extract.

Table 4. Temperature effect on the corrosion rate and inhibitory efficiency of AISI 304 stainless steel in H_2SO_4 in the presence and absence of the AW acid extract.

Temperature / ºC	**Blank**	**1 g L^{-1}**		**2 g L^{-1}**	
	$v_{corr,0}$ (mg cm^{-2} h^{-1})	**v_{corr} (mg cm^{-2} h^{-1})**	**I.E. (%)**	**v_{corr} (mg cm^{-2} h^{-1})**	**I.E. (%)**
(22 ± 2)	0.9165	0.2019	77.9	0.1034	88.7
(32 ± 2)	1.535	0.9157	40.3	0.4972	67.6
(42 ± 2)	2.338	1.674	28.4	0.8314	64.4
(52 ± 2)	4.445	4.312	2.99	1.937	53.4

Table 4 shows the results of the temperature effect on the inhibitory efficiency of the extract. The corrosion rates of the stainless steel in free and inhibited acidic media increased as the temperature increased, although the addition of the extract reduced the corrosion rate of stainless steel for all temperatures, indicating that the extract adsorbs onto the steel surface, acting as an inhibitor of corrosion reactions.

The inhibitory efficiency of the AW decreased with increasing temperature, likely due to thermic agitation, which promotes the adsorption–desorption instability of the inhibitory molecules at the metallic surface [4].

As the temperature increases with the addition of the AW acid extract, the number of adsorbed molecules decreases, as demonstrated by the reduced inhibitory efficiency of the samples. This behavior indicates that the adsorption is probably physical in nature. The apparent activation energy can be calculated by adjusting the values in equation 11, i.e., the Arrhenius equation [9]:

$$\ln v_{corr} = \frac{-E_a}{RT} + \ln A \quad (11)$$

where v_{corr} is the corrosion rate at different temperatures, E_a is the apparent activation energy, R is the molar gas constant, T is the absolute temperature (K), and A is the frequency factor. The apparent activation energy can be calculated by the angular coefficients of the ln v_{corr} vs. 1/T plot, in the presence and absence of the AW acid extract (Figure 4).

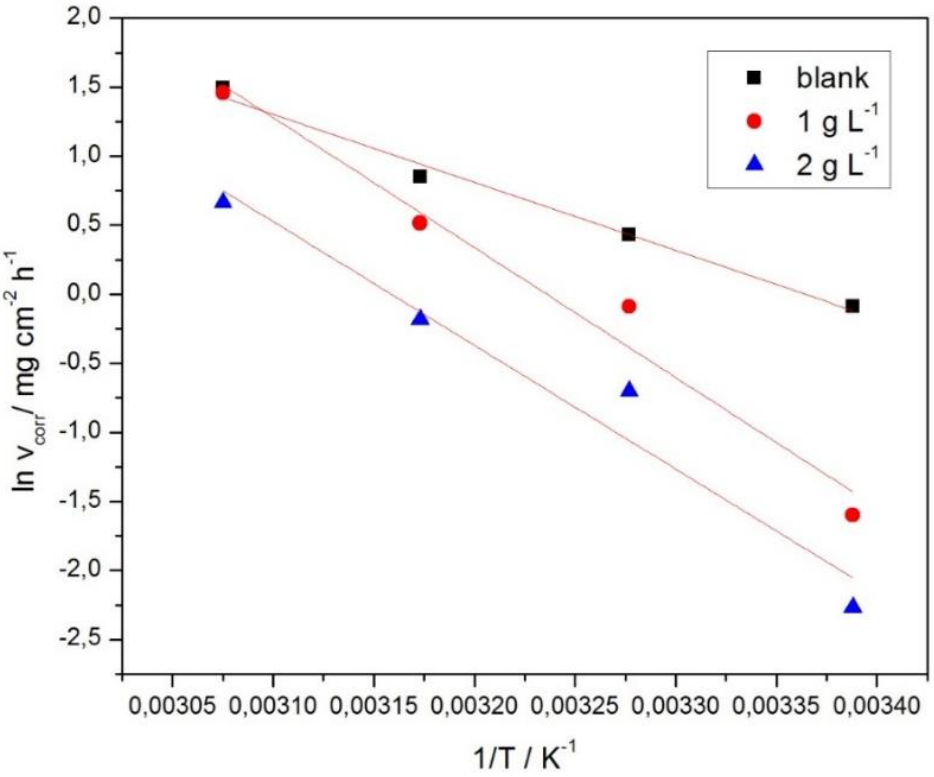

Figure 4. Arrhenius plot of AISI 304 stainless steel in 1.5 mol L^{-1} H_2SO_4 in the presence and absence of the AW acid extract.

Table 5 presents the apparent activation energy obtained from Figure 4.

Table 5. Apparent activation energy of the AISI 304 stainless steel immersed in 1.5 mol L^{-1} H_2SO_4 in the presence and absence of the AW acid extract.

Sample	**E_a / kJ mol^{-1}**
Blank	41.02
1 g L^{-1} AW acid extract	78.21
2 g L^{-1} AW acid extract	74.48

It is noted that the activation energy barrier increased with the addition of 1 g L^{-1} of the AW acid extract, indicating that a physical adsorption between the components of the extract and stainless steel was taking place. The same behavior was observed at 2 g L^{-1} of the AW extract. The physical adsorption of the molecules occurred through electrostatic interactions between the charged inhibitor molecules and the charged metallic surface, which decreased the protection capability as the temperature increased. This result is consistent with the decrease in the inhibitory efficiency as the temperature increased [4].

3.3. Surface analysis

The surface morphology after the immersion, in different concentrations, of the AW acid extract is presented in Figure 5. The steel surface is uniform, with small grooves resulting from the process of metal preparation (Figure 5A). When the metal is immersed in the 1.5 mol L^{-1} H_2SO_4 solution for 2 h, the oxidation reactions of the metal occur widely throughout the surface, resulting in the image shown in Figure 5B, where it is possible to observe the rough surface. When the AW acid extract is added to the medium, the intensity of the reactions is decreased, presenting only a few points of localized corrosion (Figure 5C). The similarity of Figures 5A and 5C indicates the efficiency of the extract as a corrosion inhibitor for stainless steel in H_2SO_4.

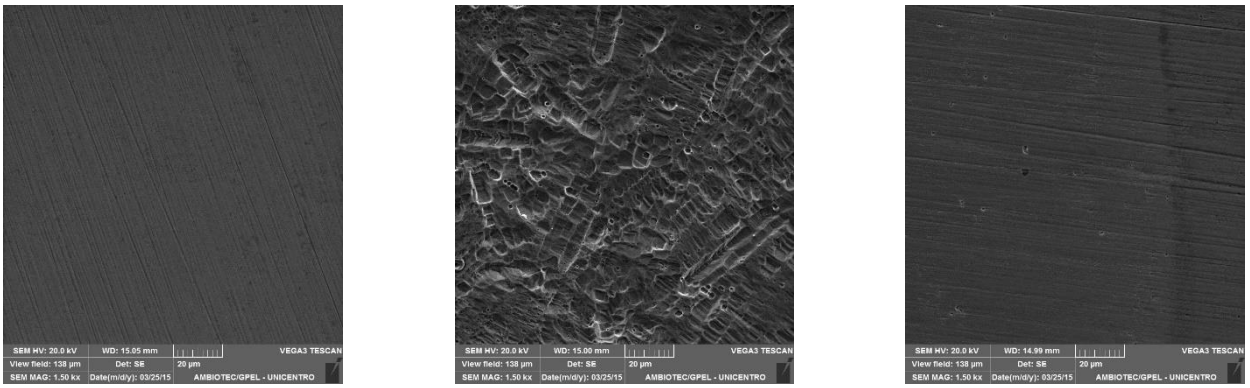

(A) (B) (C)

Figure 5. SEM images of AISI 304 stainless steel: (A) before immersion, (B) after immersion in H_2SO_4, and (C) after immersion in H_2SO_4 containing 5 g L^{-1} of AW acid extract (1500X increase).

The SEM images are correlated with the gravimetric results, indicating that the acid extract acts as a corrosion inhibitor for stainless steel in H_2SO_4.

Table 6 presents the chemical composition of the metallic samples obtained by EDS.

With the addition of 5 g L^{-1} of the AW acid extract, there is an increase in the availability of the constituent elements of the alloy (iron, chromium, and nickel). A layer of adsorbed molecules is formed, protecting the metallic surface and making the corrosive process less severe [29].

The lower quantities of iron, chromium, and nickel observed in the non-immersed samples are related to the formation of a passive film of chromium and nickel oxides and hydroxides in the stainless steel; this does not occur in the presence of the inhibitor [2].

Table 6. Chemical composition of the AISI 304 stainless steel samples obtained by EDS mapping.

Element	% / m/m		
	AISI 304 stainless steel	**AISI 304 stainless steel in 1.5 mol L^{-1} H_2SO_4**	**AISI 304 stainless steel in 1.5 mol L^{-1} H_2SO_4 + 5 g L^{-1} AW extract**
C	1.98	3.33	1.32
O	18.0	14.7	14.6
Si	0.35	0.36	0.36
Cr	15.5	16.0	16.3
Mn	1.01	1.03	1.05
Fe	56.8	58.1	59.7
Ni	6.21	6.36	6.58

3.4. Electrochemical experiments

3.4.1. Open circuit potential

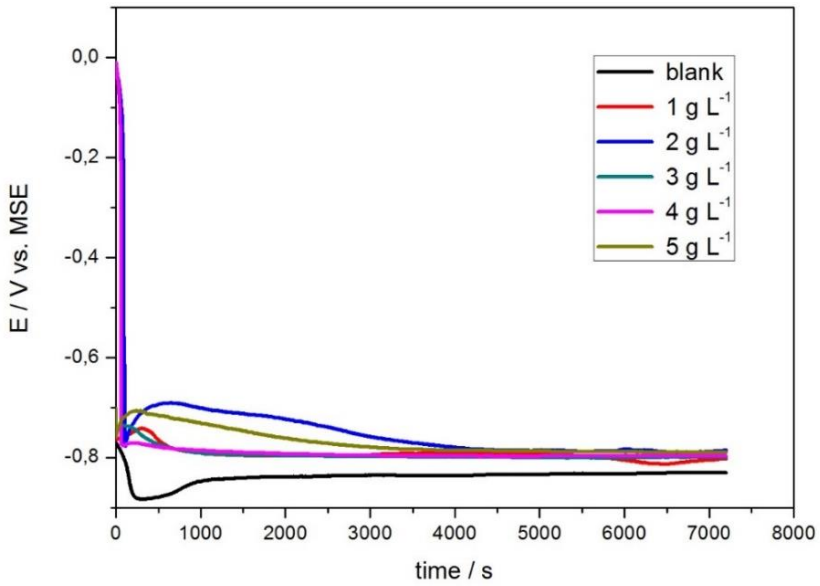

Figure 6. OCP plots of stainless steel samples in 1.5 mol L^{-1} H_2SO_4 in the presence and absence of the AW acid extract.

The OCP plots presented in Figure 6 show that for stainless steel in H_2SO_4 in the first 1000 s, the surface is more active, with an abrupt potential shift to more negative values, and then stabilizes in approximately -830 mV. This behavior indicates that there is an improvement in the oxide's layer with time.

With the addition of the AW acid extract, the behavior is quite the same, with the initial abrupt shift in the negative direction, and then the stabilization of the OCP in more positive potentials as compared to the blank. The addition of the AW acid extract improves the surface over time and acts as a corrosion inhibitor [8].

3.4.2. Potentiodynamic polarization

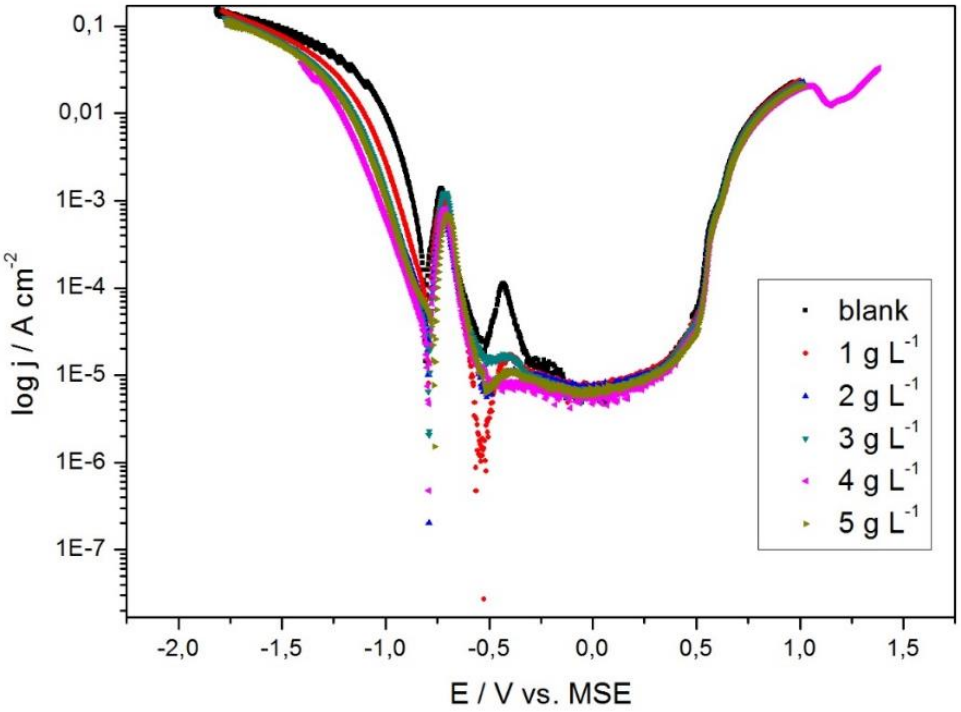

Figure 7. Polarization curves obtained for AISI 304 stainless steel in 1.5 mol L^{-1} H_2SO_4 in the presence and absence of the AW acid extract with a 1 mV s^{-1} scanning rate.

Figure 7 presents the polarization curves of AISI 304 stainless steel. The cathodic region promoted the hydrogen evolution reaction and consequent removal of the oxide layer formed during the OCP stabilization. At a potential of approximately – 880 mV/MSE, the anodic reactions occurred. The oxide layer reacted, thus presenting two active regions. The first is related with the oxides, while the second is related with the sensitization of the stainless steel [3]. Then, the current suddenly decreased due to the formation of a thin insulating layer, likely composed of chromium and iron sulphates. The current remained passive until the potential reached approximately 500 mV/MSE, where the passive film broke and the anodic reactions of the metal occurred.

The addition of the AW extract promoted a shift in the initial potential to more positive values and a decrease in the cathodic currents. The first active region was unchanged with the AW acid

extract; however, the second active region presented lower current densities in the presence of the inhibitor, showing that the extract inhibited the stainless steel sensitization process. The anodic currents in the passivation region retained the same behavior with the addition of the AW extract.

The data shown in Table 7 show that the addition of the AW acid extract to the reaction medium promoted a decrease in the corrosion current density (j_{corr}) and an increase in the polarization resistance of stainless steel samples, suggesting that the corrosion process is inhibited by the addition of the extract, as indicated in other studies [4,9,30]. There was a change of the cathodic coefficient (β_c) with its increase in the presence of the AW acid extract. Besides, the anodic coefficient decreased very little with the addition of the extract. This behavior suggests that the compounds of the AW acid extract adsorbed onto the surface promote the inhibition by a blocking effect, which is a characteristic of mixed-type inhibitors [30,31], likely changing the cathodic mechanism reaction on the uncovered surface.

Table 7. Electrochemical parameters obtained by potentiodynamic polarization of AISI 304 stainless steel in 1.5 mol L^{-1} H_2SO_4 in the presence and absence of the AW acid extract.

	blank	**1 g L^{-1}**	**2 g L^{-1}**	**3 g L^{-1}**	**4 g L^{-1}**	**5 g L^{-1}**
OCP (mV)	-830	-802	-788	-799	-797	-789
β_a (mV/dec)	65	33	43	41	42	51
- β_c (mV/dec)	123	160	171	165	159	175
$E_{corr, calc}$ (mV)	-787	-780	-783	-780	-792	-782
$E_{corr, obs}$ (mV)	-807	-792	-791	-790	-792	-779
j_{corr} (µA/cm²)	229.0	108.4	64.76	61.71	30.48	65.97
Corrosion rate (mm/year)	2.52	1.19	0.715	0.681	0.336	0.728
R_p (kΩ)	85.43	118.1	247.0	244.3	505.1	276.3
I. E. (%)	-	52.6	71.7	73.0	86.7	71.2

The study on the inhibition of the corrosion of steel reactions in 1 mol L^{-1} HCl with 2 g L^{-1} of *Salvia officinalis* leaves presented an efficiency of 96%. The studied waste presented a maximum inhibitory efficiency of 86.7% using the polarization data, indicating that natural compounds can be used to substitute synthetic organic compounds, such as azoles [6]. The results obtained by polarization experiments agreed with the gravimetric experiments.

3.4.3. Electrochemical impedance spectroscopy

Figures 8 and 9 present the Nyquist diagrams and Bode diagrams, respectively.

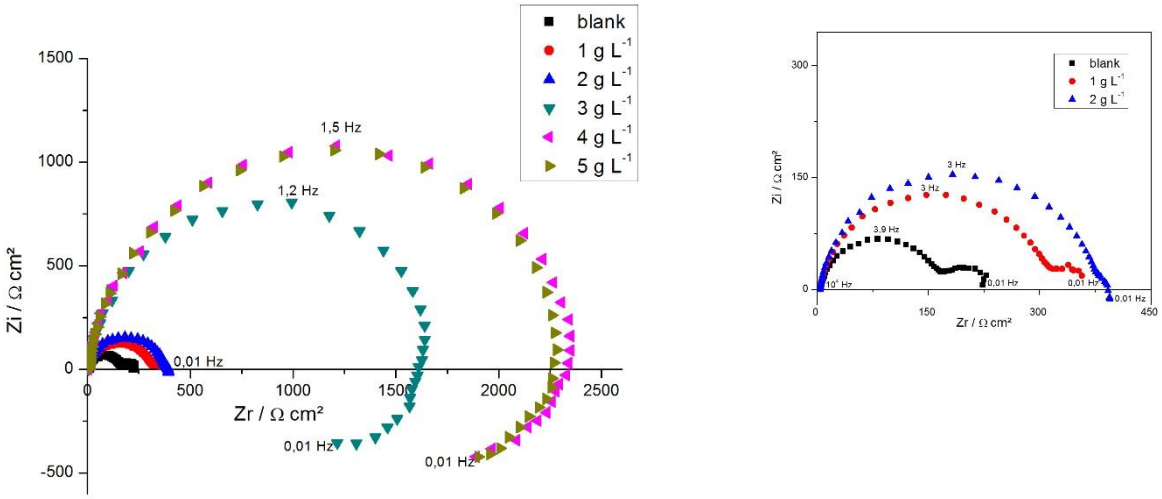

Figure 8. (A) Nyquist diagrams of AISI 304 stainless steel obtained in 1.5 mol L^{-1} H_2SO_4 in the presence and absence of the AW acid extract; (B) Extension of the 0 to 300 **Ω** cm² impedance region.

Figure 8A-B illustrates two well-defined capacitive loops of stainless steel in H_2SO_4 in the absence and presence of 1 g L^{-1} and 2 g L^{-1} of the AW acid extract. The first capacitive loop can, at high frequencies, be attributed to the time constant of the charge transfer and the double layer capacitance, while the second loop can be attributed to the relaxation of the adsorbed intermediates, which could be $[FeOH]_{ads}$, from the anodic iron dissolution, and $[FeH]_{ads}$, from the hydrogen evolution reaction, as reported in the literature [4,13,32].

It is important to note that in strong acidic solution and in the potential region near the OCP, both anodic iron dissolution and hydrogen evolution occur simultaneously on the electrode surface [32]. The extract molecules block the metallic surface, inducing the desorption of these intermediate species and decreasing the second capacitive loop size with the inhibitor concentration. For higher extract concentrations, the first capacitive loop increases 100 times while the second capacitive loop disappears, being replaced by an inductive loop [7]. The observed change in the cathodic coefficient (β_c) suggests that the intermediate species is $[FeH]_{ads}$.

The intersection of the semicircle with the real axis at higher frequencies corresponds to the value of the ohmic resistance (R_s) of the solution. The value of the charge transfer resistance (R_{ct}) was obtained by the diameter of the first capacitive loop, and the double layer capacitance (C_{dl}) was obtained from equation 12 [4,13]. The R_{ct} value is a measurement of electron transfer across the surface and is inversely proportional to the corrosion rate.

$$C_{dl} = \frac{1}{2\pi f_{max} R_{ct}} \quad (12)$$

where f_{max} is the frequency value when the imaginary impedance reaches its maximum. Table 8 summarizes the electrochemical parameters obtained by EIS.

Table 8. Electrochemical parameters for stainless steel in 1.5 mol L^{-1} H_2SO_4 in the presence and absence of the AW acid extract.

[AW] / g L^{-1}	R_s / Ω cm²	R_{ct} / Ω cm²	f_{max} / Hz	C_{dl} / µF cm^{-2}	I.E / %
0	5.17	165	3.98	242	-
1	4.68	375	3.16	134	56.0
2	4.23	376	3.16	133	56.1
3	4.32	1654	1.25	76.9	90.0
4	4.71	2356	1.58	42.7	92.9
5	5.08	2289	1.25	55.6	92.8

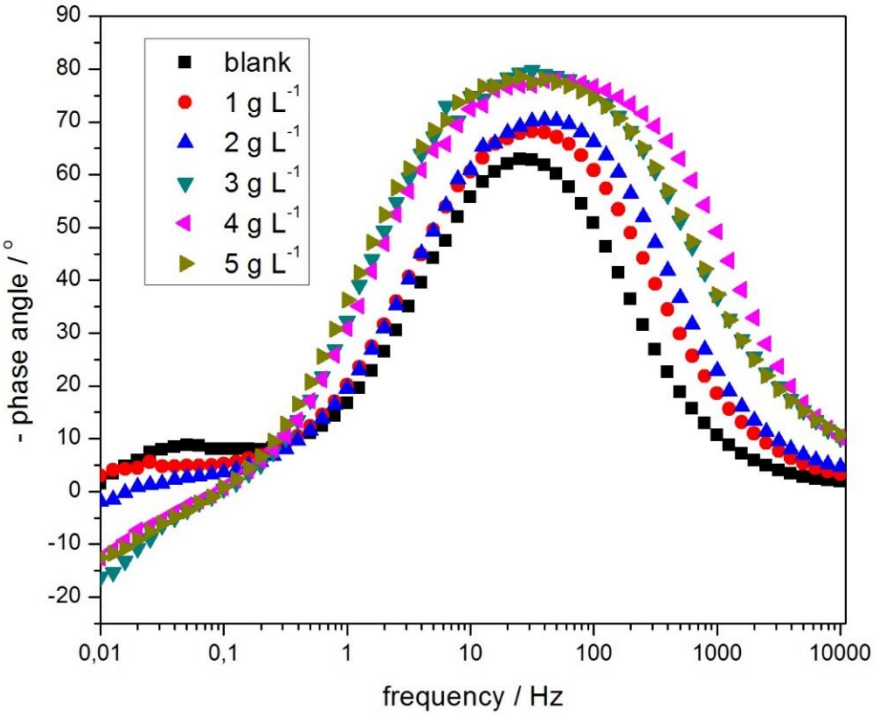

Figure 9. Bode diagrams of AISI 304 stainless steel obtained in 1.5 mol L^{-1} H_2SO_4 in the presence and absence of the AW acid extract.

It can be observed from Table 8 that with the addition of the AW acid extract, the R_s values had the same behavior. However, the R_{ct} values increased, indicating that the addition of the AW acid extract promoted surface blocking, making the charge transfer difficult. The addition of the AW extract also promoted the decrease of the double layer capacitance values. These values can be attributed to the adsorption of the extract compounds onto the steel surface, promoting the inhibition of the corrosion reactions. Similar behavior was obtained for carbon steel in HCl, as reported in the literature [4,9,13].

When benzotriazole is used as an inhibitor in 2 mol L^{-1} H_2SO_4, similar behavior is noted, as demonstrated by Rodrigues [8]. Both benzotriazole and the addition of the AW acid extract increased the stainless steel R_{ct}; in other words, the waste can be used as a substitute for synthetic organic compounds for corrosive control in stainless steel.

Figure 9 indicates that the stainless steel samples immersed in 1.5 mol L^{-1} H_2SO_4 presented a single time constant in the 10000-10 Hz region associated with the charge transfer process. This behavior remains the same with the addition of the AW acid extract. Higher phase angles were obtained for the samples containing the AW acid extract, suggesting that the oxide formed in these conditions is more protective [33].

4. CONCLUSIONS

- The AW acid extract is an efficient inhibitor for AISI 304 stainless steel in H2SO4.
- The gravimetric results indicate that increasing the concentration of the extract in the reaction medium increases inhibitory efficiency. The temperature increase of the solution decreased inhibitory efficiency, suggesting physical adsorption of the compounds at the metallic surface.
- The apparent activation energy of stainless steel in H_2SO_4 increased with the addition of 1 g L^{-1} and 2 g L^{-1} AW acid extract, indicating that the extract acts through physical adsorption.
- Electrochemical measurements of the OCP showed that the addition of AW improves the stainless steel surface. EIS measurements showed an increase in R_{ct} with the addition of AW and a desorption of an intermediate species. PP measurements showed that AW is an efficient inhibitor, decreasing the corrosion current densities. All electrochemical measurements indicated that the extract acts mainly as a mixed-type inhibitor.
- The system obeys a Langmuir isotherm.

ACKNOWLEDGMENTS

The authors thank CNPq, CAPES, Fundação Araucária, FAU – Fundação de Apoio ao Desenvolvimento da Unicentro and FINEP for their financial support.

References

1. A.S. Fouda and A.S. Ellithy, *Corros. Sci.*, 51 (2009) 868.
2. A. Pardo, M.C. Merino, A.E. Coy, F. Viejo, R. Arrabal and E. Matykina, *Corros. Sci.*, 50 (2008) 780.
3. M. Abdallah, *Mater. Chem. Phys*., 82 (2003) 786.
4. J.C. da Rocha, J.A.C.P. Gomes and E. D'Elia, *Corros. Sci*., 52 (2010) 2341.
5. N. Soltani, N. Tavakkoli, M. Khayatkashani, M. R. Jalali and A. Mozavidade, *Corros. Sci*., 62 (2012) 122.
6. X. Li, S. Deng and H. Fu, *Corros. Sci.*, 62 (2012) 163.
7. A.B. Silva, S.M.L. Agostinho, O.E. Barcia, G.G.O. Cordeiro and E. D'Elia, *Corros. Sci*., 48 (2006) 3668.
8. P.R.P. Rodrigues, O benzotriazol como inibidor de corrosão para ferro e ligas ferrosas em meios de ácido sulfúrico, Universidade de São Paulo. São Paulo, Brasil, (1997).
9. S.S.A.A. Pereira, M.M. Pêgas, T.L. Fernández, M. Magalhães, T.G. Schöntag, D.C. Lago, L.F. de Senna and E. D'Elia, *Corros. Sci*., 65 (2012) 360.
10. M. Tussolini, C. Spagnol, E.C. Gomes, M.T. Cunha and P.R.P. Rodrigues, *Rev. Esc. Minas,* 60 (2007) 41.

11. A.M. Abdel-Gaber, B.A. Abd-El-Nabey, I.M. Sidahmed, A.M. El-Zayady and M. Saadawy, *Corros. Sci.*, 48 (2006) 2765.
12. F. Zucchi and I.H. Omar, *Surf. Technol*., 24 (1985) 391.
13. V.V. Torres, R.S. Amado, C.F. Sá, T.L. Fernández, C.A.S. Riehl, A.G. Torres and E. D'Elia, *Corros. Sci.*, 53 (2011) 2385.
14. T.F. Souza, M. Magalhães, V.V. Torres and E. D'Elia, *Int. J. Electrochem. Sci.*, 10 (2015) 22.
15. A.Y. El-Etre, *Appl. Surf. Sci*., 252 (2006) 8521.
16. P.S. Melo, K.B. Bergamaschi, A.P. Tiveron, A.P. Massarioli, T.L.C. Oldoni, M.C Zanus, G.E. Pereira and S.M. de Alencar, *Ciência Rural*, 41 (2011) 1088.
17. M.S.B. Sousa, L.M. Vieira, M.J.M. Silva and A. Lima, *Ciência Agrotec*., 35 (2011) 554.
18. M. Saadawy, *Anti-Corrosion Methods Mater*., 4 (2015) 220.
19. A.A. Melo, M. Manfio and C.S. da Rosa, *Rev. Bras. Prod Agroind.*, 18 (2016), 91.
20. L.A.C. Matos, P.R.P. Rodrigues, E. D'Elia, N.L. Boschen, G.A.R. Maia, M.C. Taborda, C. Cristostimo, M.T. Cunha and E.P. Banczek, BR 2016 023590 1, 2016.
21. American Society for Testing and Materials. ASTM-G31-72: standard practice for laboratory immersion corrosion testing of metals. In: Anonymous, Annual Book of ASTM Standards. Philadelphia: American Society for Testing and Materials; 2004.
22. N. Soltani, N. Tavakkoli, M.K. Kashanu, A. Mozavizadeh, E.E. Oguzie and M.R. Jalali, *Ind Eng Chem.*, 20 (2014) 3217.
23. V.V. Torres, G.B. Cabral, A.C.G da Silva, K.C.R. Ferreira and E. D'Elia, *Quim. Nova*, 39 (2016) 423.
24. H.K. Chung, W.H. Kim, J. Park, J. Cho, T.Y. Jeong and P.K. Park, *J. Ind. Eng. Chem*., 28 (2015) 241.
25. C.A.P. Almeida, Caracterização do lutito barro branco e avaliação de sua capacidade como adsorvente de corantes usando o azul de metileno como modelo. Universidade Federal de Santa Catarina, Florianópolis, Brasil (2005).
26. M. Behpour, S.M. Ghoreishi, M.K. Kashani and N. Soltani, *Mater. Corros*., 60 (2009) 895.
27. P.C. Okafor, M.E. Ikpi, I.E. Uwah, E.E. Ebenso, U.J. Ekpe and S.A. Umoren, *Corros. Sci*., 50 (2008) 2310.
28. Y. Liu, *Colloids Surfaces A Physicochem. Eng. Asp*., 274 (2006) 34.
29. P. Zhao, Q. Liang and Y. Li, *Appl. Surf. Sci*., 252 (2005) 1596.
30. F.S. de Souza and A. Spinelli, *Corros. Sci*., 51 (2009) 642.
31. S. Deng and X. Li, *Corros. Sci*., 55 (2012) 407.
32. A.A. Hermas and M.S. Morad, *Corros. Sci*., 50 (2008) 2710.
33. M. Mehdipour, B. Ramezanzadeh and S.Y. Arman, *J. Ind. Eng. Chem*., 21 (2015) 318.